

Europa's surface water ice crystallinity and correlations between lineae and hydrate composition. J. R. Berdis¹ and J. R. Murphy² and N. J. Chanover², ¹Johns Hopkins Applied Physics Laboratory, Laurel, MD, jodi.berdis@jhuapl.edu, ²New Mexico State University, Las Cruces, NM.

Introduction: Surface composition and evidence for cryovolcanic activity on Jupiter's moon, Europa, can provide insight into the properties and composition of the subsurface ocean based on the potential transport of material between the subsurface ocean and the icy surface. A combination of hydrated brines, hydrated sulfuric acid, and water ice are proposed to be present on Europa's surface and likely reproduce features in spectra of Europa's surface [1-6].

Crystallinity. The relative fractions of amorphous and crystalline water ice ("crystallinity") are influenced by a) the thermal relaxation of amorphous into crystalline water ice; b) the conversion of crystalline to amorphous water ice due to charged particle bombardment from interactions with Jupiter's magnetic field; c) vapor deposition of water ice as outbursted plume material (either in the crystalline or amorphous form) falls back onto the surface; and d) any additional cryovolcanic activity such as diapirs that could warm the ice and convert amorphous into crystalline water ice. In this study we aim to identify the spatial distribution of the crystallinity for two locations near the equator and south pole on the leading hemisphere.

Study Goals. This investigation uses a spectral mixture approach to identify the abundances of pure materials, or endmembers (including amorphous and crystalline water ice, hydrated sulfuric acid, and brines), that exist across Europa's surface as observed by the Galileo NIMS instrument.

We built upon previous work by Dalton et al. [6] by (1) introducing amorphous water ice into the spectral mixture analysis process alongside crystalline water ice; (2) using updated optical constants for amorphous and crystalline water ice [7]; (3) including a more diverse cryogenic reference spectral library [8]; and (4) analyzing the spatial variation of endmember abundances across each NIMS observation, rather than averaging multiple pixels together to represent a specific type of terrain/material. We used hyperspectral image data from the Galileo NIMS instrument [9], synthetic amorphous and crystalline water ice spectra at multiple grain sizes produced using Hapke theory [10-12], and cryogenic laboratory reference spectra. We implemented the spectral mixture analysis technique to identify abundances of endmember materials within each NIMS pixel separately. This work has been accepted for publication in the Planetary Science Journal.

Data & Methods: We used two hyperspectral data cubes from the Galileo NIMS instrument, 15e015 (7.3°N, 114°W, 3.0 km/pixel) and 17e009 (63°S, 120°W, 1.5 km/pixel). The Drizzlecomb Linea crosses 15e015, and the Adonis Linea crosses 17e009. Due to the presence of these lineae tracks, we predicted that the composition of the cubes would reflect alterations made to the surface due to subsurface material upwelling through surface lineae as a result of subsurface ice movement [13]. Lineae are associated with red, non-water ice, hydrated material, though the question of whether that material is of endogenic or exogenic origin is still an active discussion [14].

Reference Spectra. We used optical constants and employed the Hapke surface-scattering radiative transfer model [10-12] to produce synthetic spectra of Europa's surface amorphous and crystalline water ice for multiple grain sizes [7]. However, optical constants of our reference brine materials for the specific temperatures and pressures that exist on Europa's surface are not currently available in the literature. Therefore, we used reflectance spectra from Dalton et al. [15], Dalton [16], Carlson et al. [13], and Hanley et al. [8] for our brine materials.

Spectral Mixture Analysis. In order to determine the abundances of each of our endmembers in the NIMS image cubes, we performed a Non-Negative Least Squares spectral mixture analysis on each pixel separately. This method assumes that a single observed spectrum is the combination of various pure material spectra, or endmembers, weighted by their respective fractional abundances that exist in that single observation.

Results: The image cubes do not extend substantially in the latitudinal direction, and they consist of long strips rather than maps, since the observations were acquired in Long-Spectrometer Mode and consisted of a single ground track. For this reason, we assessed the results from the spectral mixture analysis in longitude space only, and abundances for pixels at varying locations in latitude were plotted at the same longitude.

Figure 1 provides the crystallinity results from the 15e015 cube, where crystallinity is the fraction of the total water ice that is in the crystalline form. We estimated a crystallinity of ~35%; this is consistent with spectroscopically-derived crystallinities of ~30% for the full-disk leading hemisphere [17]. The calculated crystallinity as derived spectroscopically is

therefore independent of the methodology used, i.e., Berdis et al. [17] made use of the 1.65/1.5 μm band area ratios, whereas this study implemented a spectral mixture analysis on the full 1.2-2.4 μm range of the NIR spectrum. This therefore provides a check on the spectroscopically derived crystallinities calculated in Berdis et al. [17], and strengthens the argument that particle flux and thermophysical modeling alone cannot reproduce the crystallinity present on Europa's leading hemisphere.

We found that comparatively there was more crystalline water ice at the equator than at the south pole. The higher overall abundance of amorphous water ice over crystalline water ice in both cubes could be a result of the depth into the surface that is probed by NIR observations. Hansen & McCord [18] suggested that deeper than ~ 1 mm (i.e., the depth probed by NIR observations), water ice on Europa is predominantly crystalline, however nearly all of the water ice above a depth of ~ 1 mm is amorphous. Results from our study indicate that there is more radiation-altered amorphous water ice existing at the equator up to a depth of ~ 1 mm than previously thought, suggesting that radiation alteration is overpowering the efficiency of thermal relaxation converting amorphous into crystalline water ice.

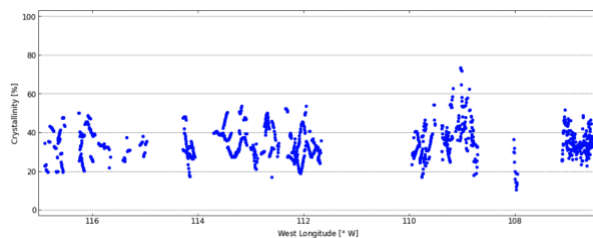


Figure 1. Distribution of crystallinity across the 15e015 NIMS cube near the equator. The mean crystallinity of all pixels is $\sim 35\%$.

Figure 2 provides a subset of abundance profiles for the 17e009 cube, specifically MgCl_2 , H_2SO_4 , and 250 μm amorphous water ice. At 124°W , the MgCl_2 abundance formed a double peak feature; a single peak feature also existed at 121.5°W . These two features are mirrored in the H_2SO_4 abundance profile, where increases in the MgCl_2 abundances correlate to decreases in the H_2SO_4 abundances; a double trough feature occurs at 124°W and a single trough feature occurs at 121.5°W in the H_2SO_4 abundance profile. We hypothesize that these locations correlate to the locations of bands that have recently undergone alteration in the form of MgCl_2 -abundant material upwelling from below the surface, and in the process, reduced the signal of radiolytically-produced H_2SO_4 that was present on the surface. This is consistent with previous results; Carlson et al. [13] found that the

abundance of H_2SO_4 was lower within lineae compared to the nearby material. The double peak structure could arise from a doublet ridge or triple band surface feature, though it is difficult to identify the structure of Adonis Linea at this location due to the low resolution of the SSI imagery. Higher resolution imaging of the surface at this location is needed to assess the correlation of double ridge structures with the abundances of H_2SO_4 and MgCl_2 .

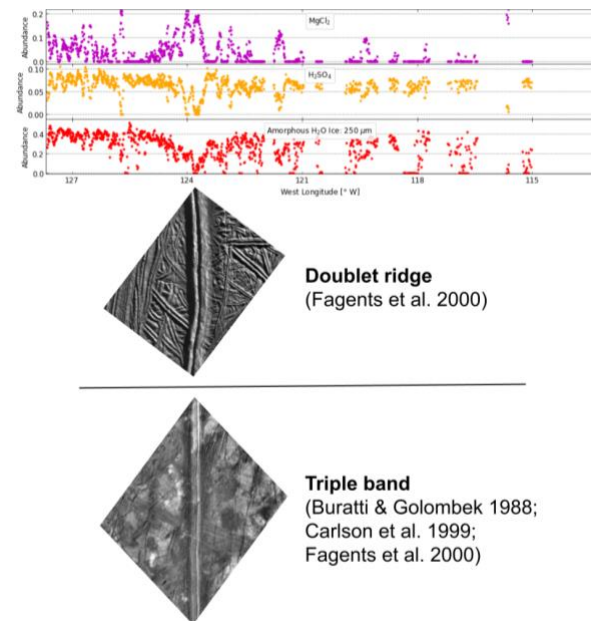


Figure 2. Abundance profiles across the 17e009 NIMS cube for MgCl_2 , H_2SO_4 , and 250 μm amorphous water ice. Images of a doublet ridge and triple band are shown to demonstrate possible surface features that could cause the abundance patterns located at ~ 124 - 125°W . Images courtesy of Fagents et al. [19].

Acknowledgments: This study was funded by NASA under Grant 80NSSC17K0408 issued through the NASA Education Minority University Research Education Project (MUREP) as a NASA Harriett G. Jenkins Graduate Fellowship through the Advanced STEM Training and Research (ASTAR) Fellowship. Galileo NIMS data were provided by the PDS Cartography and Imaging Sciences Node.

References: [1] McCord et al. (1998) *JGR*, 103, 8603. [2] McCord et al. (1999) *JGR*, 104, 11827. [3] Carlson et al. (1999) *Science*, 286, 97. [4] McCord et al. (2002) *JGR (Planets)*, 107, 5004. [5] Shirley et al. (2010) *Icarus*, 210, 358. [6] Dalton et al. (2012) *JGR (Planets)*, 117, E03003. [7] Mastrapa et al. (2008) *Icarus*, 197, 307. [8] Hanley et al. (2014) *JGR (Planets)*, 119, 2370. [9] Carlson et al. (1992) *SSRv*, 60, 457. [10] Hapke (1981) *JGR*, 86, 3039. [11] Hapke (1984) *Icarus*, 59, 41. [12] Hapke (1986) *Icarus*, 67, 264. [13] Carlson et al. (2005) *Icarus*, 177, 461. [14] Carlson et al. (2009) *Europa's Surface Composition*, 283. [15] Dalton et al. (2005) *Icarus*, 177, 472. [16] Dalton (2007) *GRL*, 34, L21205. [17] Berdis et al. (2020) *Icarus*, 341, 113660. [18] Hansen & McCord (2004) *JGR (Planets)*, 109, E01012. [19] Fagents et al. (2000) *Icarus*, 144, 54.